Journal of Food Engineering 184 (2016) 10–20

Contents lists available at ScienceDirect

Journal of Food Engineering

journal homepage: www.elsevier.com/locate/jfoodeng

Effects of freezing on microstructure and rehydration properties of freeze-dried soybean curd

Nathdanai Harnkarnsujarit [a, b, *], Kiyoshi Kawai [c], Manabu Watanabe [a], Toru Suzuki [a]

[a] Department of Food Science and Technology, Tokyo University of Marine Science and Technology, 4-5-7, Konan, Minato-ku, Tokyo, Japan
[b] Department of Packaging and Materials Technology, Faculty of Agro-Industry, Kasetsart University, 50 Ngam Wong Wan Rd, Lat Yao, Chatuchak, Bangkok 10900, Thailand
[c] Department of Biofunctional Science and Technology, Graduate School of Biosphere Science, Hiroshima University, 1-4-4 Kagamiyama, Higashi-Hiroshima, Hiroshima, Japan

ARTICLE INFO

Article history:
Received 22 October 2015
Received in revised form
18 February 2016
Accepted 25 March 2016
Available online 30 March 2016

Keywords:
Freezing
Microstructure
Rehydration
Freeze-drying
Soybean curd

ABSTRACT

Ice crystallization controls the microstructure and subsequent mass transport of water in freeze-dried food matrices. This study investigated the effects of freezing on the microstructure and rehydration properties of porous, freeze-dried soybean curd. Soybean curd was prefrozen at various freezing conditions (−20 °C, −50 °C, −90 °C and in Liq.N_2) prior to freeze-drying. Scanning electron microscopy showed a correlation between pore morphologies and freezing temperatures. The patterns of ice formed in the 3-D matrices were revealed using X-ray computed tomography. The decreased freezing temperature from −20 °C to −90 °C gave clearer needle ice formation in parallel with heat transfer resulting in a sponge-like structure after rehydration with a corresponding wall thickness of 2.9–21.8 μm. Conversely, the Liq.N_2 freezing gave very fine ice crystals which effectively retained the fresh-soybean curd structure and color upon rehydration. Cracking increased with decreased freezing temperatures which also accelerated solid loss during rehydration. A correlation between the pore morphology (i.e. pore diameter and 1st-order rehydration kinetics) was observed. Cluster analysis revealed that freezing at −20 °C and −50 °C changed the color; whereas, freezing at −90 °C and with Liq.N_2 effectively preserved the color of the rehydrated soybean curd. The results clearly demonstrated a process-structure-function relationship in freeze-drying which can be effectively utilized in the structural design of freeze-dried food materials.

1. Introduction

Food structure has a pronounced effect on the transport properties of foods (e.g., diffusivity, permeability and thermal conductivity). The physical structure of a food material is of fundamental importance in the developing field of food materials science (Krokida and Philippopoulos, 2005). The porous structures of dehydrated materials play a paramount role in the modeling of mass transfer applications in dehydrated foods (Marabi and Saguy, 2004). Food processing, such as freezing and dehydration, contribute to various structural changes of food matrices such as protein aggregation, phase separation of colloidal systems and the crystallization of water and solutes leading to the modification of functional properties, for example the stability of nutrients and hydration properties of freeze-dried matrices (Rhim et al., 2011; Harnkarnsujarit and Charoenrein, 2011; Voda et al., 2012). The microstructure of food is a key parameter in understanding food properties and stability.

The food model selected for the present study was soybean curd or tofu, which forms a gel as a result of the denaturation of soy protein. The principal components of soybean proteins are 11S (glycinin) and 7S (β-conglycinin). In their native state, soy proteins do not form a gel; therefore, the proteins are heat-denatured and then coagulated to form soybean curd with water, soy lipids and other constituents trapped in its gel network (Keshun, 1997). Proteins provide various functional properties of foods including water holding capacity; however, several food processes possibly modify and affect the functional properties of protein networks. Drying (including freeze-drying) potentially promotes protein aggregation

* Corresponding author. Department of Packaging and Materials Technology, Faculty of Agro-Industry, Kasetsart University, 50 Ngam Wong Wan Rd, Lat Yao, Chatuchak, Bangkok 10900, Thailand.
E-mail address: nathdanai.h@ku.ac.th (N. Harnkarnsujarit).

http://dx.doi.org/10.1016/j.jfoodeng.2016.03.014
0260-8774/

(Wang et al., 2010) and therefore, possibly affects the functional properties of protein networks including their hydration characteristics.

Freeze-drying retains the high quality of foods and bioproducts including the appearance, nutrients, flavor and high rehydration capacity. The process consists mainly of freezing and dehydration under reduced pressure. The ice nucleation and growth during freezing directly impact the morphologies of the freeze-dried matrices (Petzold and Aguilera, 2009) namely pore size and membrane/network thickness. A successful freeze-drying process results in highly porous, dehydrated matrices with a high rehydration capacity, which is an important property of freeze-dried foods for consumption or used in various industrial applications such as instant soups and ready-to-eat products. The most important property of freeze-dried food products is the ability to properly rehydrate after liquid reconstitution using water or milk.

Rehydration is a process of moistening dry material, mostly, using abundant amounts of water, which causes adsorption of the water and leaching of solutes (Lewicki, 1998). Rapid rehydration with the least solid loss is required for a better quality of rehydrated products. Rehydration properties have been extensively investigated in plant materials, including fruits and vegetables (Krokida and Marinos-Kouris, 2003; Witrowa-Rajchert and Lewicki, 2006; Marques et al., 2009), while only a few studies have demonstrated the rehydration characteristics of protein-based food matrices (Babić et al., 2009).

The rates of reactions or the kinetic parameters describe how fast a reaction proceeds and are favored for the comparison of different factors. Numerous researchers have compared the kinetics of water uptake as influenced by food matrices due to different dehydration methods such as air-drying, freeze-drying and vacuum-drying (Farkas and Singh, 1991; Krokida and Marinos-Kouris, 2003; Witrowa-Rajchert and Lewicki, 2006; Marques et al., 2009) and dehydration processes (Lin et al., 1998; Marabi et al., 2004; Marabi and Saguy, 2004; Babić et al., 2009; Rhim et al., 2011; Voda et al., 2012). However, very limited research has focused on the influence of varying the freezing process on the kinetics of water uptake of freeze-dried matrices. In addition, the previously reported data about the influence of the freezing process on the rehydration properties of freeze-dried foods are inconsistent (Farkas and Singh, 1991; Kuprianoff, 1962; Babić et al., 2009; Rhim et al., 2011; Voda et al., 2012). Rhim et al. (2011) reported that freeze-dried rice porridge frozen at −5 °C absorbed water most rapidly, followed by −20 °C, −70 °C and −40 °C, respectively. Generally, the rehydration ratio increased with an increase in the freezing temperature except for freezing at −40 °C which was probably due to the prolonged time for ice crystal formation and the slow freezing rate in the −40 °C system (Rhim et al., 2011). Kuprianoff (1962) and Babić et al. (2009) demonstrated that slow-frozen samples had higher rehydration percentages than fast-frozen samples due to larger holes. These aforementioned authors suggested that large ice crystals formed by slow freezing were preferable in the freeze-drying process since they promoted the reconstitution of the freeze-dried products. Conversely, Farkas and Singh (1991) reported that slower freezing caused poorer rehydration in freeze-dried, white chicken meat which was possibly due to the aggregation of muscle protein, especially cross-linking of actomyosin. Accordingly, contradictory conclusions regarding the freezing effects on the rehydration capacity of freeze-dried foods were found based on these previous investigations.

The objective of this study was to determine the effects of freezing conditions on microstructure and their subsequent impacts on the rehydration properties including the kinetics of water uptake, solid leaching, microstructural properties and surface color of freeze-dried, soybean curd matrices. Various freezing conditions, namely at −20 °C, −50 °C, −90 °C and in liquid nitrogen (Liq.N_2), were applied to control the microstructural properties of the solids. This study emphasized the importance of the process-structure-function relationship in freeze-dried systems and would be beneficial in the design structures of freeze-dried food matrices for desirable rehydration properties.

2. Materials and methods

2.1. Freezing and freeze-drying

Soybean curds or tofu (10 × 10 × 3 cm) were purchased in the same lot from a local market in Tokyo (moisture content 88.67% w.b.). The soybean curd samples were cut into 15 × 15 × 5 mm. Approximately 100 pieces of samples were placed between two aluminum trays (approximately 15 × 22 × 2.5 cm) prior to pre-freezing in conventional freezers at −20 °C, −50 °C and −90 °C for 20 h as well as using liquid nitrogen freezing. The liquid nitrogen freezing was performed by placing the aluminum trays and samples in a polystyrene foam box. The liquid nitrogen was poured into the bottom of the foam box as well as on the upper trays to freeze the soybean curd for 15 min which was then transferred to storage at −90 °C. The freezing profiles of the soybean curd samples were recorded at 0.1 s intervals using type-T thermocouples (copper-constantan) connected to a data logger (Memory HiLOGGER LR8431, HIOKI E.E. Corporation, Nagano, Japan). The thermocouples were inserted at the core of the tofu samples and placed at identical distances between the aluminum plates. The freezing properties as shown in Table 1 were calculated from triplicate samples. After prefreezing, all soybean curd samples were transferred to storage at −90 °C for 24 h prior to freeze-drying. The frozen soybean curd samples were freeze-dried at below 100 Pa with a step-increased, shelf-temperature of 5 °C every 6 h from −40 °C to 20 °C using a freeze-dryer (Kyowac, Kyowa Vacuum Engineering Co., Ltd., Tokyo, Japan). The vacuum was released with ambient air. The freeze-dried samples were stored in an evacuated desiccator containing P_2O_5 to remove residual water prior to the measurement and considered as having “zero” water content.

2.2. Scanning electron microscopy

Microstructural properties of freeze-dried materials were measured using a scanning electron microscope (FEI Quanta-250 SEM, FEI Company, Czech Republic). Freeze-dried soybean curd samples were sectioned with a sharp blade and placed on the SEM stub using two-sided, adhesive carbon tape prior to sputter-coating with platinum using an E-1030 ion sputter (Hitachi Science Systems, Ltd., Japan). The specimens were transferred to the SEM and the images were collected under low vacuum (100Pa) at a 10 kV accelerated voltage and spot size of 6.0 with a large field detector (LFD). The SEM images were captured at 100× magnification.

The SEM images were analyzed for image pixels which were further converted to a physical size using the scale bar of the SEM micrographs. The pore diameter and wall thickness of freeze-dried soybean curd were randomly evaluated from 23 areas of each image. The average length of the maximum and minimum diameter in each pore was determined as the pore diameter and the wall thickness was measured as the distance between two pores.

The wall thickness of the freeze-dried matrices was derived as described by Harnkarnsujarit et al. (2012) with an assumption of the formation of spherical ice crystals to derive the number of ice crystals formed at the maximum freeze-concentration of the systems that was maintained throughout freeze-drying. This presumed freezing of water to form an unfrozen phase with 80% solutes and 20% water (Roos and Karel, 1991; Roos, 1993) An

Table 1
Freezing and microstructural properties of freeze-dried tofu prefrozen under various freezing conditions.

Freezing condition	Freezing properties [a]		Microstructural properties [b]					
	Cooling rate, R_c (°C/min)	Freezing time, T_f (min)	Pore diameter			Wall thickness		
			Average (μm)	Min-max (μm)	CV [c]	Average (μm)	Min-max (μm)	CV [c]
−20 °C	0.72 ± 0.05a	64 ± 5a	119 ± 24a	76–160	0.199	11 ± 3a	6.5–21.8	0.327
−50 °C	1.51 ± 0.55b	19 ± 1b	65 ± 11b	41–90	0.180	8 ± 2b	4.4–10.2	0.237
−90 °C	2.18 ± 0.77b	9 ± 1c	48 ± 6c	35–57	0.119	5 ± 1c	2.9–7.3	0.233
Liq.N_2 (−196 °C)	50.09 ± 4.62c	N/A	15 ± 3d	10–20	0.170	2± 0d	1.2–3.6	0.262

Different letters indicate a significant difference within the same column ($p \leq 0.05$).
[a] Freezing properties determined from freezing curve. Values shown are mean ± SD (n = 3).
[b] Microstructural properties determined from SEM images. Values shown are mean ± SD (n = 23).
[c] Coefficient of variation (CV) = SD/mean.

expansion of the spheres based on the density of ice (0.917 kg/m^3) was used to derive the frozen radius of the same number of spheres on which a proportion of the unfrozen fluid (14% initial weight) could form a surface coverage to a final radius with a half thickness of the interparticle walls.

2.3. X-ray CT

Three-dimensional microstructural properties of freeze-dried soybean curd were determined using a Skyscan 1172 X-ray micro-computed tomography system (X-ray CT, Bruker, Kontich, Belgium). The freeze-dried soybean curd was wrapped in cling film to prevent water adsorption and mounted on a rotational plate. The X-ray voltage and current was 54 kV and 100 μA, respectively. A CCD camera with 2000 × 1332 pixels was used to record the transmission of the conical X-ray beam through all samples. The distance source-object-camera was adjusted to produce images with a pixel size of 9.01 μm. The matrices were scanned for 180° using a rotational step of 0.2° with 10 random movements and an exposure time of 1480 ms with two frames averaging contributing to the scan time of 125 min. Three-dimensional reconstruction of samples was created by stacking two-dimensional tomographs from a total of 800–1000 slices with a slice spacing of 0.013 mm using the reconstruction NRecon software (Version 1.6.8.0, Bruker, Kontich, Belgium). A ring artifact reduction (set to 7) and beam hardening correction (52%) were performed with the NRecon software. At least two freeze-dried specimens were subjected to the X-ray CT measurement.

2.4. Rehydration of freeze-dried soybean curd

Freeze-dried soybean curd was individually packed into filter bags and immersed in distilled water (500 ml) at 25 °C for interval times of 0.5, 1, 1.5, 2, 3, 4, 5, 7, 10, 15, 25, 40, 60, 90, 120 and 180 min. Triplicate rehydrated samples were removed from the filter bags and gently blotted with tissue paper to remove excess water on surface. The samples were oven-dried at 105 °C for 24 h using a DOV-300P programmed control oven (AS ONE, Osaka, Japan). The weight of freeze-dried soybean curd was determined gravimetrically using a digital balance (±0.001 g; FX-300i, A&D Company, Limited, Tokyo, Japan). The water contents (W, g/g dried solids) as a function of rehydration time (t, min) were calculated using Eq. (1):

$$W_t = \frac{M_t - M_0}{M_{d,t}} \quad (1)$$

where M_t is the weight of the rehydrated sample, M_0 is the weight of freeze-dried solids before rehydration and M_d is the weight of the oven-dried solids after rehydration (dried mass).

The experimental data on water uptake were fitted to first-order kinetics (Eq. (2)) and the rate constants were derived. An initial rapid and thereafter a slower water uptake were observed to 10 min; therefore, the rate constants were derived for below 10 min and above 10 min of rehydration.

$$\ln\left[\frac{W_t - W_e}{W_0 - W_e}\right] = -kt \quad (2)$$

where W_e is the equilibrium water content (g/g dried solids), k is the derived rate constant and t is the rehydration time (min). The rehydration rate is determined as the slope of the falling rate of rehydration curve (Krokida and Marinos-Kouris, 2003).

Rehydration capacities (R) were calculated from Eqs. (3) and (4):

$$R_B = \frac{Weight\ of\ rehydrated\ sample}{Weight\ of\ freeze-dried\ solids\ before\ rehydration} \quad (3)$$

$$R_D = \frac{Weight\ of\ rehydrated\ sample}{Weight\ of\ oven-dried\ solids\ after\ rehydration} \quad (4)$$

where here R_B and R_D are the rehydration capacities based on the dried weight before rehydration, and after rehydrated with subsequent oven-drying, respectively.

The solid leaching (L) during rehydration was determined at time intervals and was expressed as % solid loss from Eq. (5):

$$L_t = \frac{M_0 - M_{d,t}}{M_0} \times 100 \quad (5)$$

where L_t is the percentage of solid leaching at an interval rehydration time (t), M_0 is the weight of freeze-dried solids before rehydration and M_d,t is the weight of the oven-dried solids after rehydration (dried mass) at an interval rehydration time (t).

The experimental data were fitted to a second-order polynomial equation and the trend lines were generated for each system using Microsoft® Excel 2010 (Microsoft Japan Company, Limited, Tokyo, Japan). The rehydration experiments were performed in triplicate.

2.5. Fluorescence microscopy

The microstructural properties of the rehydrated soybean curd samples were monitored using a BZ-9000 fluorescence microscope (Keyence Corporation, Osaka, Japan). The freeze-dried soybean curd samples were rehydrated in distilled water for 60 min at 25 °C. The sample preparation for microscopic measurements included specimen embedding, cryo-sectioning and fluorescence-dye staining with rhodamine B which shows affinity to protein domains in food matrices (Peighambardoust et al., 2010). The rehydrated samples

were sectioned (3 × 5 × 5 mm) using a sharp blade and deep frozen in liquid-nitrogen-cooled-isopentane for at least 3 min prior to embedding in FSC 22 frozen section media (Leica Microsystems K.K., Tokyo, Japan) and then storing at −80 °C. The samples were cryo-sectioned using a Leica CM1850 cryostat, Leica Microsystems Nussloch GmbH, Nussloch, Germany) into samples with 8 μm thickness and placed on micro slide glass using a cryofilm type IIC (Leica Microsystems K.K., Tokyo, Japan). Paraformaldehyde (2%v/v) was dropped to fix the specimens for 1 min prior to washing with distilled water. The specimens were stained with 1.0% (w/v) rhodamine B in 2-methoxyethanol (Wako Pure Chemical Co., Ltd., Osaka, Japan) for 1 min and gently washed in excess water prior to mounting on micro slide glass with Fluoromount™ aqueous mounting medium (Sigma-Aldrich Japan G.K., Tokyo, Japan). The microstructural properties of fresh soybean curd were also determined using the same preparation procedures. Two to five soybean curd specimens were prepared and subjected to the microscopic analysis.

2.6. Color measurement

The surface color of fresh, freeze-dried and rehydrated soybean curd samples was determined using a spectrophotometer CM-600d (Konica Minolta Sensing Inc., Osaka, Japan). The samples were gently blotted with tissue paper to remove water on the surface prior to the color measurements. The SCE values of L*, a* and b* were obtained from 6 soybean curd samples after calibration using a standard white reflector. The differences between fresh soybean curd and freeze-dried/rehydrated samples were reported as ΔE.

$$\Delta E = \sqrt{(L^*_1 - L^*_2)^2 + (a^*_1 - a^*_2)^2 + (b^*_1 - b^*_2)^2} \quad (6)$$

A 3-D scatter plot of the experimental data was drawn using the SPSS 17.0 software for Windows (SPSS Inc., Chicago, IL, USA).

2.7. Statistical analysis

The color properties (L*, a* and b*) were subjected to cluster analysis as well as analysis of variance (ANOVA) with Duncan's multiple range test at 95% confidence intervals ($p < 0.05$) for mean comparison. The statistical analysis among cooling rates was determined using the Kruskal-Wallis test based on an assumption of non-normal distribution or non-similar variances. The statistical measurements were carried out using the SPSS 17.0 software for Windows. Error was reported in terms of the standard deviation (SD) or as the coefficient of variation (CV; CV = SD/mean) to compare the relative variation between different freezing conditions.

3. Results and discussion

3.1. Freezing properties

Soybean curd samples were frozen at various prefreezing conditions (−20 °C, −50 °C, −90 °C and Liq.N_2) prior to freeze-drying. The freezing curves of soybean curd are shown in Fig. 1. The initial slope of the freezing curve indicates the cooling rate and determines the rate of water nucleation; whereas, the freezing time suggests the time it takes for the freezable water present in food to freeze (López-Leiva and Hallström, 2003). Steeper slopes was observed for lower temperature freezing indicating increased cooling rates and decreased freezing times which suggest less ice growth in the period (Table 1). In addition, the decreased freezing temperatures from −20 °C to −90 °C gave a linearly increasing

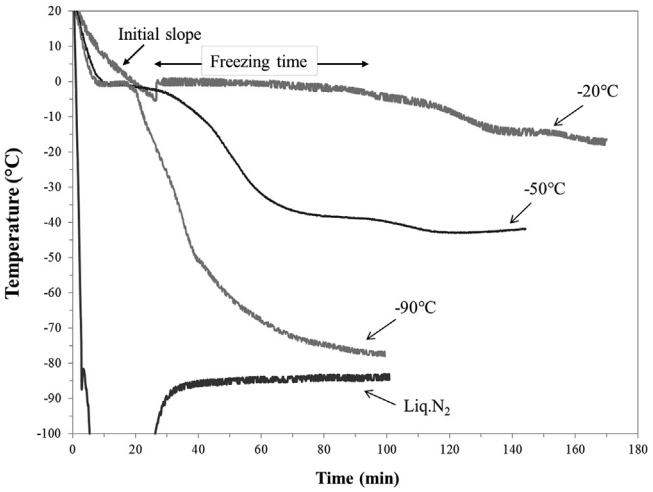

Fig. 1. Freezing profile of tofu prefrozen under various freezing conditions (−20 °C, −50 °C, −90 °C and in liq.N_2). Liquid nitrogen freezing involved prefreezing soybean curd samples in liquid nitrogen for 15 min prior to transfer to a −90 °C freezer.

cooling rate from 0.72 to 2.18 °C/min; whereas a freezing temperature of −196 °C with Liq.N_2 freezing gave very rapid cooling with a cooling rate of 50.02 °C/min. The experimental cooling rate and freezing time correlated well with a power law model (Eq. (7)):

$$T_f = 29.823 R_c^{-1.326} \ (R^2 = 0.91) \quad (7)$$

where T_f and R_c are the freezing time (min) and cooling rate (°C/min), respectively. Liq.N_2 freezing sharply decreased the sample temperature. The simultaneous release of latent and sensible heat occurred during rapid cooling using Liq.N_2. An instant rise followed by an immediate drop in temperature was observed in the freezing profile of the Liq.N_2 system. The reason for such a temperature fluctuation around −80 to −90 °C was unclear. However, it could possibly be attributed to noise or the release of latent heat of crystallization. Nevertheless, the presence of temperature fluctuation at such a low temperature could be due to a late response by the data logger and should not be regarded as 'nucleation temperature'. The ice nucleation in the Liq.N_2 system took place followed by a sharp temperature drop to −196 °C which restricted ice growth (Fig. 1). The results indicated ice formation under all freezing conditions which influenced the microstructural properties of the freeze-dried matrices as explained later.

3.2. Microstructural properties of freeze-dried matrices

The SEM and X-rayCT images showed the interconnected solid networks and embedded pores previously occupied by ice crystals during prefreezing and vacated as a result of ice sublimation (Fig. 2). The microstructural properties (pore diameter and wall thickness) from image analysis of the SEM micrographs are shown in Table 1. Freezing at −20 °C produced the largest pore size; whereas the smallest pores were clearly seen under the Liq.N_2 freezing conditions (Table 1 and Fig. 2a). Ice sublimation left the pores embedded in the matrices which determined ice nucleation and growth during freezing and freeze-drying. The lower freezing temperatures and hence higher cooling rates increased the rate of ice nucleation concurrently with limited ice growth during freezing. The nucleation rate defines the number of ice crystals; while the rate of heat and protein diffusion away from the point of nucleation defines the ice crystal size (O'Brien et al., 2004); therefore, large numbers of small ice crystals were formed during

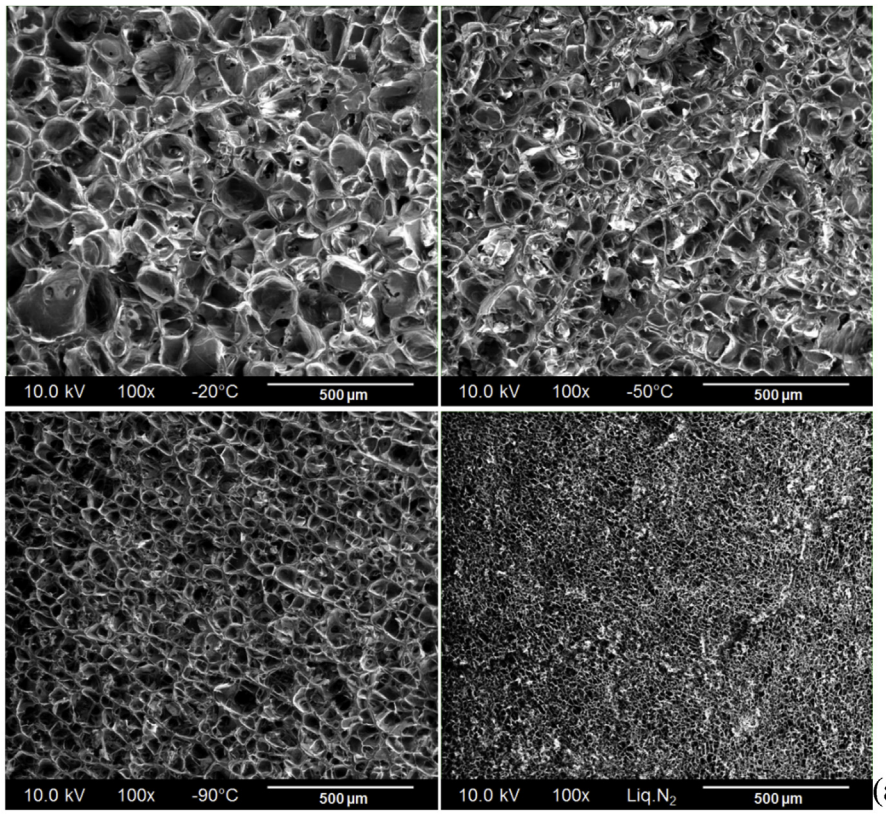

Fig. 2. Microstructures of freeze-dried tofu prefrozen under various freezing conditions (−20 °C, −50 °C, −90 °C and in liq.N_2) prior to freeze-drying: (a) SEM images of transaxial structures at 100× and (b) X-rayCT images of coronial structures. The binary color of X-ray CT images indicates different planes of solids.

fast freezing which contributed to the smaller pore sizes after ice sublimation.

Soybean curd samples (5-mm thickness) were placed between aluminum trays and frozen; therefore, the heat transfer primarily proceeded through the metal surfaces. Accordingly, X-ray CT images visualized the direction of ice formed in the soybean curd matrices (Fig. 2b). It was clear that Liq.N_2 freezing produced very fine ice crystals dispersed in food matrices (Fig. 3). Freezing at −50 °C and −90 °C formed the needle-like ice in a parallel direction to the heat transfer from the metal layers with the size depending on the cooling rate and freezing time. Conversely, freezing at −20 °C formed a non-directional, oval ice shape. The results indicated that fast freezing at −50 °C and −90 °C caused gradient temperatures within the matrices and nucleation possibly took place from the surface followed by subsequent water transfer to the previously formed ice interface causing needle-shaped structures. In contrast, slow freezing effectively reduced the temperature gradients and the nucleation was likely distributed within the matrices; however, the slow cooling increased ice growth and, therefore, large ice crystal size were formed which also disrupted the protein network of soybean curd.

Moreover, the faster cooling rate from 0.72 to 2.18 °C/min produced a more homogeneous pore morphology (pore size and wall thickness) as indicated by a smaller CV value (Table 1) which agreed with previous studies (Kang et al., 1999; Ma and Zhang, 1999). A faster cooling rate reduced ice growth which caused non-uniform ice crystal formation. However, very rapid freezing of Liq.N_2 (R_c 50.09 °C/min) increased the CV values which indicated less pore homogeneity. The rapid quench freezing process results in space-variable and time-variable heat transfer through the systems, leading to non-uniform nucleation and growth of ice crystals and, subsequently, matrix heterogeneity (O'Brien et al., 2004). The results showed a non-linear correlation between the cooling rate of soybean curd and the average pore size of freeze-dried solids (Fig. 4). Voda et al. (2012) quantified the pore size of freeze-dried carrots and observed a correlation between the average pore size and freezing rates that followed a power law model with increased freezing rate resulting in a smaller pore size.

The smaller pore size was concurrent with a thicker membrane forming under the lower temperature freezing conditions. Fig. 4 shows that the experimental and theoretical thickness of protein networks in soybean curd increased linearly with increasing pore diameter in agreement with previous investigation in carbohydrate systems (Harnkarnsujarit et al., 2012).

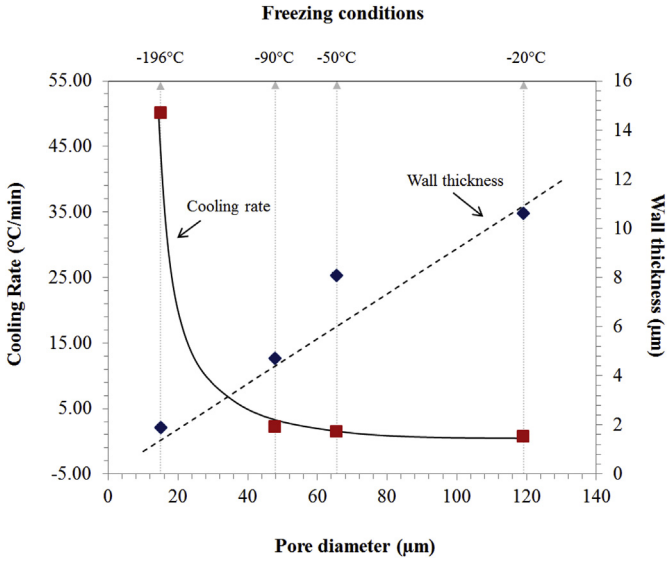

Fig. 4. Relationship between freezing conditions, cooling rate (■), wall thickness (◆) and pore size of freeze-dried tofu solid prefrozen at −20 °C, −50 °C, −90 °C and in liquid nitrogen (−196 °C). The wall thickness for freeze-dried solids correlated with 86% surface coverage of spherical ice crystals by the unfrozen fluid giving the theoretical wall thickness shown as a dotted line.

3.3. Rehydration kinetics

Rehydration is a major desired property of freeze-dried foods. The rehydration capacities of soybean curd prefrozen under various freezing conditions are shown in Table 2. The decreased freezing temperatures clearly gave an increased rehydration capacity. R_D had slightly higher values than R_B due to the solid leaching from matrices during rehydration.

The water sorption of freeze-dried soybean curd during

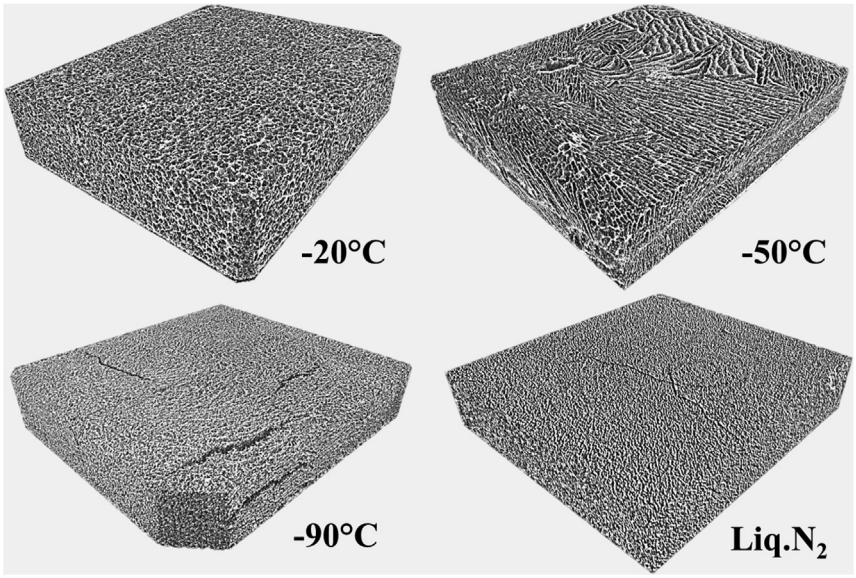

Fig. 3. Three-dimensional structures of freeze-dried tofu prefrozen under various freezing conditions (−20 °C, −50 °C, −90 °C and in liq.N_2) prior to freeze-drying.

Table 2
Rehydration capacity and solid loss equation of freeze-dried tofu prefrozen under various freezing conditions (−20 °C, −50 °C, −90 °C and in liq.N_2).

Freezing condition	Rehydration capacity (R) [a]		Solid loss	
	R_D (g/g dried solids)	R_B (g/g before rehydration)	Calculated equation	R^2
−20 °C	3.87 ± 0.02a	3.35 ± 0.03a	$y = -0.00008x^2 + 0.1136x + 3.4407$	0.9792
−50 °C	4.30 ± 0.33b	3.69 ± 0.38a	$y = -0.0001x^2 + 0.1005x + 3.3897$	0.9595
−90 °C	5.06 ± 0.11c	4.38 ± 0.09b	$y = 0.00007x^2 + 0.0697x + 3.0474$	0.9804
Liq.N_2 (−196 °C)	6.26 ± 0.05d	5.24 ± 0.03c	$y = -0.0006x^2 + 0.1448x + 2.491$	0.9528

Values shown are mean ± SD (n = 3).
Different letters indicate a significant difference within the same column ($p \leq 0.05$).
[a] Values were calculated at equilibrium water content from a rehydration time of 180 min.

rehydration is shown in Fig. 5. All systems showed a sharp increase in the water content up to 10 min, and thereafter it slowed down until reaching equilibrium. The rapid moisture uptake was due to surface and capillary suction (Lewicki, 1998). Previous research indicated that water imbibition into freeze-dried materials took place by capillary flow driven by capillary pressure gradients rather than by diffusion (Marabi and Saguy, 2004; García-Pascual et al., 2006; Wallach et al., 2011). Capillary flow is due to the difference between the relative attraction of the molecules of liquid for each other and for those of solids (Datta, 2007). At the early stage of rehydration, water rapidly filled up the void spaces of the freeze-dried matrices by capillarity and, therefore, the water uptake instantaneously increased. The lower-temperature freezing and hence the smaller void space embedded in the dehydrated matrices resulted in a faster water uptake (almost instantaneously for the Liq.N_2 freezing system), due to smaller cavities which significantly led to an increased capillary flow (Datta, 2007).

The water content of the soybean curd samples was identical prior to freeze-drying and, therefore, the volume fraction of pores or void space of freeze-dried matrices were presumed to be effectively the same among the different prefreezing conditions. However, Fig. 5 clearly revealed a significant difference in the equilibrium water uptake as a result of freezing. Matrices with a smaller pore size and thinner interconnected networks exhibited higher water uptake at equilibrium (Fig. 6a). The different sizes of ice formed manipulated the solid pore diameter and hence the volume of water to fill up the void space which also depended on the attraction between the solid (soy protein) and liquid water. At an identical matrices (solid + pores) volume, a smaller pore

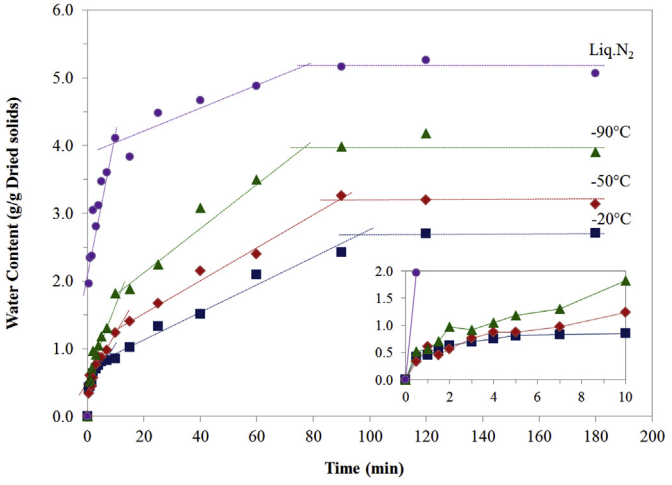

Fig. 5. Water sorption during rehydration for 180 min at 25 °C of freeze-dried tofu prefrozen at −20 °C (■), −50 °C (◆), −90 °C (▲) and in liq.N_2 (●). The symbols show average experimental data (n = 3). Dotted lines show connections within the same group of samples and guide the water sorption behavior of freeze-dried tofu. The SD bars were removed to make data points easier to see. Inset figure presents experimental data of up to 10 min rehydration with the lines connecting data within the same group.

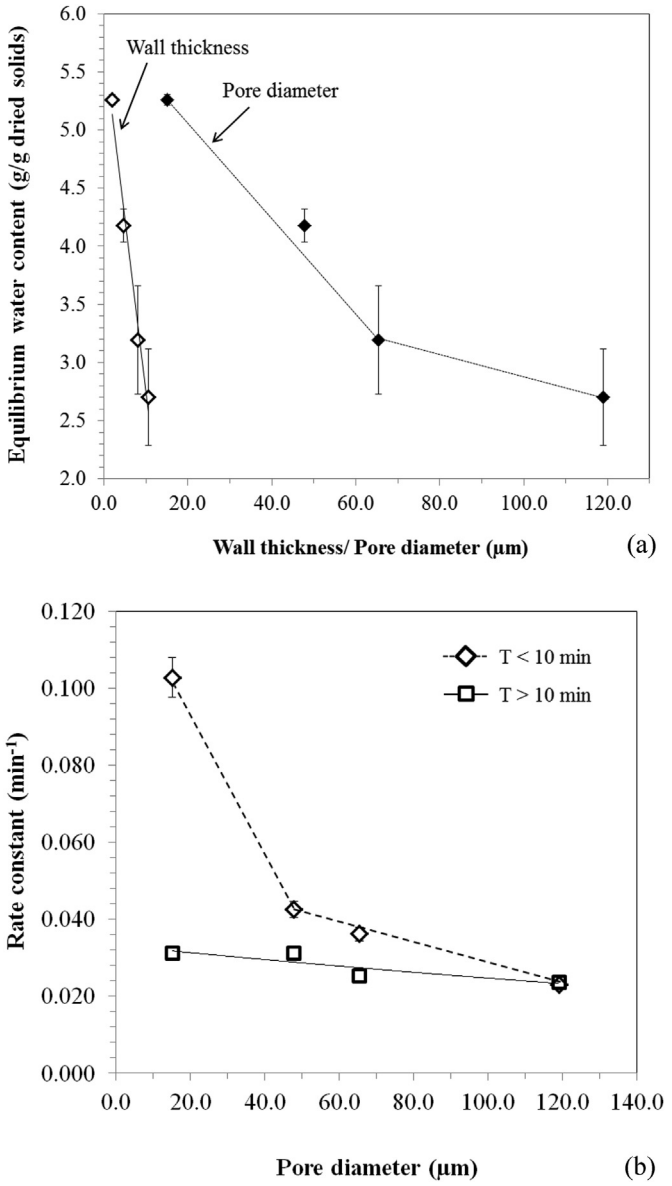

Fig. 6. Relationship between microstructure (pore diameter and wall thickness) and rehydration properties; (a) equilibrium water contents (W_e), (b) first-order rate constants (k) of water sorption below and above 10 min of rehydration (T < 10 min and T > 10 min, respectively). Lines in figures indicate connections between data points within the same groups. Average values shown (n = 3).

diameter gave a higher surface area for water adsorption. The ice crystallization expelled the denatured soy protein network and caused aggregation which subsequently formed an interconnected protein network surrounding the pores upon ice removal. Therefore, the thickness of such a network influenced the water accessibility and hydration of solids during reconstitution. The thicker solid networks formed a larger interspace of solids between adjacent pores and hence possibly hindered water accessibility, resulting in less water being available to rehydrate matrices. A slower freezing significantly reduced the equilibrium water contents which were 84.0%, 80.7%, 76.1% and 73.0% (w.b.) for the Liq.N_2, −90 °C, −50 °C and −20 °C systems, respectively. The results indicated that the thickness of the interconnected network also played a key role in the hydration of water and hence controlled the amount of equilibrium water uptake.

The experimental data were fitted to first-order kinetics and the rates of water uptake were derived (Krokida and Marinos-Kouris, 2003; Krokida and Philippopoulos, 2005; Saguy et al., 2005). An initial fast and thereafter a slower water uptake was observed from 10 min of rehydration; therefore, the rate constants were calculated at below 10 min and above 10 min, as shown in Fig. 6b. Freezing clearly affected the rates of water uptake during the former period. Faster freezing, particularly Liq.N_2 freezing, gave a more rapid water uptake as water could freely penetrate through the thin, solid networks; whereas the thicker networks (resulting from slow freezing) reduced water accessibility leading to a slower water uptake. Water moved freely through some of the large cavities but in the case of small ones, the fluid spread around cavities. Consequently, this encirclement formed air bubbles entrapped in the cavity, which is a major hindrance for fluid intrusion through cavities (Lewicki, 1998). Accordingly, the rate of water uptake decreased above 10 min which was possibly due to the formation of entrapped air bubbles inside the cavities of the small pore systems (−50 °C, −90 °C and Liq.N_2) except for the −20 °C system. The large cavities of the −20 °C system, however, enhanced faster air escape (Kuprianoff, 1962) which reduced the amount of entrapped air and allowed free water penetration through the pores.

The results showed that faster freezing led to a higher rehydration rate which was inconsistent with Babić et al. (2009) and Rhim et al. (2011). It is possible that, in these previous studies, large amounts of ice formed large amounts of open pores in the slower freezing systems which accelerated water transport during rehydration (Marabi and Saguy, 2004). Marabi and Saguy (2004) indicated that the kinetics of water uptake were influenced by the matrix porosity, throat length and the connectivity between the pores as well as the pore size distribution. A higher porosity, which determines the volume of void spaces solids, contributed to a higher rehydration capacity (Marques et al., 2009). Conversely, the thickness of the membrane was low enough for the transport of water through the pores and, therefore, the open porosity had only a minor effect in the present study. Moreover, the results indicated that the rate of water uptake varied with the rehydration time. Accordingly, the different mechanisms taking place during rehydration could also explain the contradictory results compared to other investigations.

3.4. Structures of rehydrated soybean curd

The systems frozen at −20 °C, −50 °C and −90 °C produced a sponge-like structure of hydrated soybean curd matrices. Fig. 3 shows that the freezing accelerated the aggregated soybean curd structures and increased the wall thickness. The irreversibly modified soybean curd structures with a corresponding wall thickness between 2.9 and 21.8 μm (Table 1) resulted in the sponge-like structures. The Liq.N_2 freezing effectively retained a structure similar to that of raw soybean curd material. Freezing using Liq.N_2 produced a very fine pore size of freeze-dried soybean curd; however, substantial cracking was observed after rehydration (Fig. 7). Systems prefrozen at −90 °C also showed small cracks on the soybean curd surface; whereas, no cracking was observed in the systems prefrozen at −20 °C and −50 °C. The results clearly indicated that rapid freezing increased the cracking of freeze-dried matrices in agreement with previous studies (Harnkarnsujarit and Charoenrein, 2011; Voda et al., 2012). The very rapid freezing caused water to flow out and freeze at the surface which caused shrinkage (Scherer, 1993) and formed a hard crust that prevented further internal expansion. When the internal matrix was frozen, the liquid-solid transition of water took place concurrently with the increased volume of the internal portion which subsequently cause expansion force against resistance from the surface. Consequently, the cracking occurred once the expansion force exceeded the strength of the crust during freezing (Hung, 1997; Harnkarnsujarit and Charoenrein, 2011). In addition, imbibition of water resulted in swelling of materials undergoing rehydration and fast hydration contributed to the swelling stress (Lewicki, 1998) which accelerated cracking in the low temperature freezing and hence small cavity systems.

The microstructural properties of rehydrated and non-frozen soybean curd are shown in Fig. 8. Soybean curd specimens were stained with rhodamine B which shows affinity to protein domains (Peighambardoust et al., 2010). Raw soybean curd showed highly connected networks with very fine void spaces (Fig. 8a). The freezing clearly modified and caused irreversible aggregation of protein networks contributing to the enlarged intercellular space in materials after freeze-drying and subsequent rehydration. An extensive increase in the pore size was observed under slow freezing conditions; whereas, the Liq.N_2 freezing produced only slightly larger void volumes than the non-frozen system as a result of the very fine ice crystals formed during freezing. Moreover, the liquid nitrogen freezing effectively maintained highly connected hydrated protein matrices. Conversely, disruption of the protein networks was clearly observed in systems prefrozen

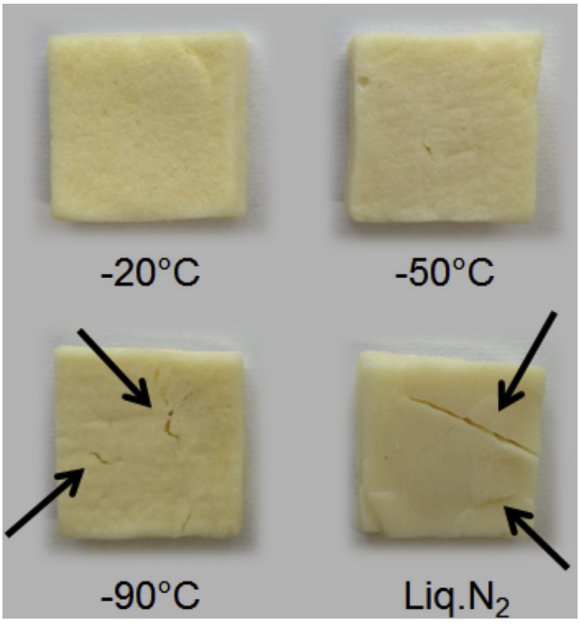

Fig. 7. Appearance of rehydrated freeze-dried tofu prefrozen at −20 °C, −50 °C, −90 °C and in liq.N_2 after reconstitution in distilled water for 10 min. Arrows indicate cracking of tofu structures.

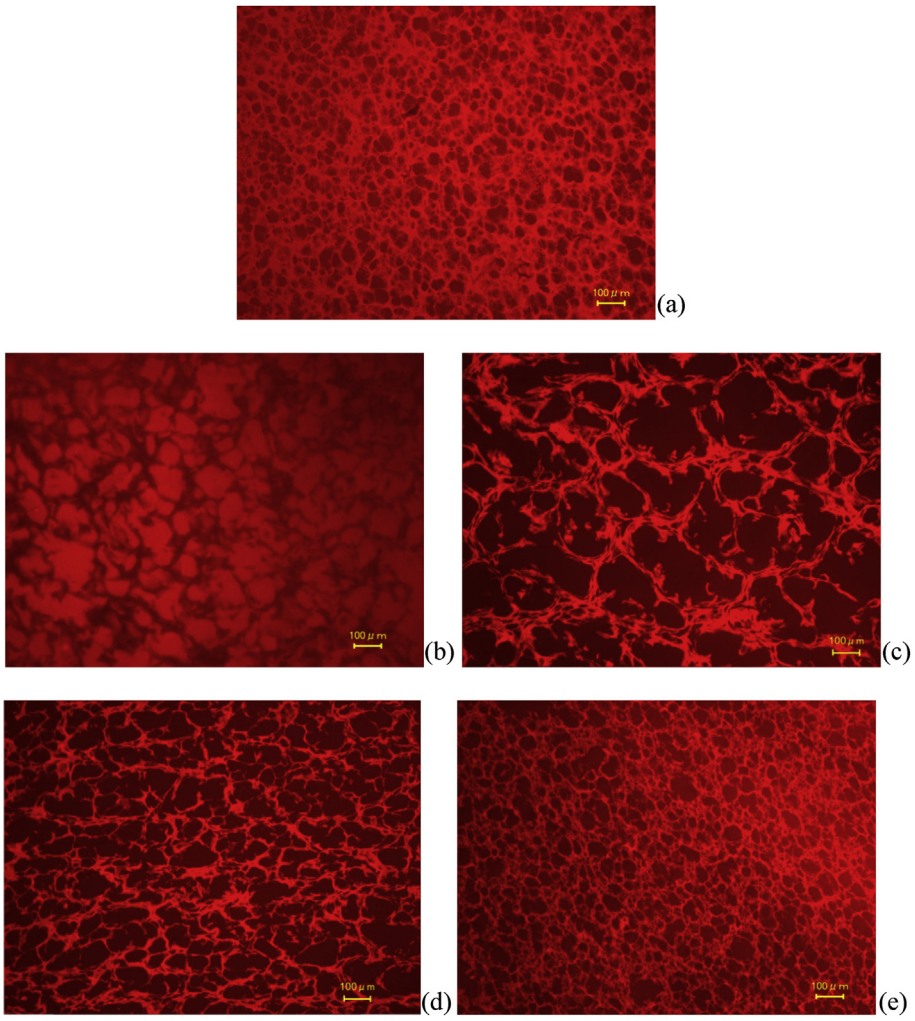

Fig. 8. Fluorescent microimages of (a) fresh and rehydrated tofu prefrozen at (b) −20 °C, (c) −50 °C, (d) −90 °C and (e) in liq.N_2 prior to freeze-drying. Samples were rehydrated in distilled water for 60 min at 25 °C.

at −20 °C, −50 °C and −90 °C. The hydration caused swelling and loosened the network proximity which reduced the matrix strength. Moreover, the large ice crystals disrupted and reduced the integrity of the protein networks. However, the highest tear was observed in −50 °C and not the −20 °C systems which could have been due to restricted water accessibility through the solids of the −20 °C systems and thus limited network swelling. The hydration caused the swelling of matrices and with the high integrity network of Liq.N_2 systems, the matrices achieved complete recovery.

3.5. Solid leaching during rehydration

Rehydration leads to water uptake and the simultaneous dissolution of water soluble solids. Fig. 9 shows the solid loss from freeze-dried soybean curd matrices during rehydration. The derived equation from a second-order polynomial equation produced the highest coefficient of determination (R^2, 0.95–0.98) in all soybean curd systems (Table 2). The water penetration through the porous matrices provoked high leaching of soluble solids, hence affecting the nutritional qualities and simultaneously the matrices' ability to imbibe water (Marabi et al., 2004). The lowest solid loss at the early stage of systems prefrozen at −20 °C was explained by the lowest water accessibility resulting from the largest pores and

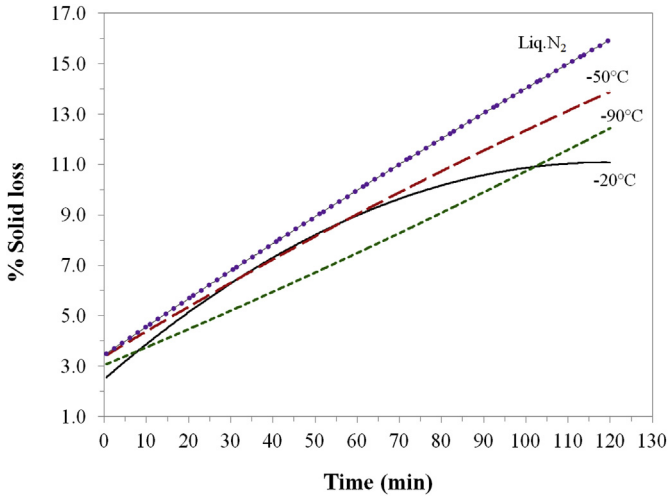

Fig. 9. Solid loss during rehydration of freeze-dried tofu prefrozen at −20 °C, −50 °C, −90 °C and in liq.N_2 for 120 min at 25 °C. The trend lines were derived from fitting the experimental data to 2nd order polynomial equations with R^2 = 0.95–0.98. The experimental values were not included to make the data easier to see.

Table 3
Color measurements (L*, a*, b* and Δ E) of fresh, freeze-dried and rehydrated tofu samples.

System	L*	a*	b*	Δ E
Fresh	88.02 ± 0.19a	4.12 ± 0.03b	20.80 ± 0.17bc	–
Freeze-dried_−20 °C	89.43 ± 0.53bc	5.29 ± 0.34cd	24.73 ± 1.46f	4.45 ± 1.17c
Freeze-dried_−50 °C	88.83 ± 0.66b	5.24 ± 0.41cd	23.85 ± 1.80ef	3.54 ± 1.51bc
Freeze-dried_−90 °C	89.95 ± 0.72c	4.90 ± 0.33c	21.61 ± 1.17cd	2.57 ± 0.31ab
Freeze-dried_Liq.N_2	95.98 ± 0.29d	2.22 ± 0.11a	10.86 ± 0.23a	12.63 ± 0.31d
Rehydrated_−20 °C	89.47 ± 0.46bc	5.42 ± 0.33d	23.36 ± 1.45ef	3.39 ± 1.02bc
Rehydrated_−50 °C	88.93 ± 0.56b	5.51 ± 0.63d	22.78 ± 2.02de	3.07 ± 1.25b
Rehydrated_−90 °C	89.96 ± 0.44c	5.34 ± 0.28d	21.38 ± 0.83cd	2.52 ± 0.16ab
Rehydrated_Liq.N_2	88.12 ± 0.50a	4.21 ± 0.30b	19.35 ± 1.20b	1.62 ± 1.08a

Different letters indicate a significant difference within the same columns ($p \leq 0.05$).
Values shown are mean ± SD (n = 6).

thickest networks; however, such systems showed a sharp increase of solid loss up to 60 min which suggested a tendency to have the highest solid loss. The large amount of ice formed in high temperature freezing systems possibly reduced the strength and integrity of the protein network and hence the hydration accelerated the leaching of water-soluble solids (e.g. amino acids and whey), particularly at the surface of the pores. Therefore, the amount of solid leaching was expected to be in the order of −20 °C > −50 °C > −90 °C as a result of the network disruption by the formation of large ice crystals. However, the very limited amount of water imbibition through the −20 °C systems after 60 min restricted the solid leaching fraction resulting in only a slight increase in the solid loss after further rehydration time. The integrity and damage of tissue was a major factor affecting the kinetics of solid leaching during rehydration in various investigations (Marabi et al., 2004; Witrowa-Rajchert and Lewicki, 2006).

Moreover, the results clearly revealed that the smallest pore matrices of Liq.N_2 freezing gave the highest degree of solid loss due to the high surface area and thin solid networks which increased hydration through the protein networks. In addition, the cracking possibly allowed higher water penetration through the solid which accelerated solute leaching.

3.6. Color properties

The color properties (L*, a* and b*) of raw, freeze-dried and rehydrated soybean curd materials are shown in Table 3. Freeze-drying significantly increased the lightness values of soybean curd in agreement with Meda and Ratti (2005). Faster freezing produced a whiter-colored freeze-dried matrix. Acevedo et al. (2008) also reported a lighter color in freeze-dried apples prefrozen in Liq.N_2 than from prefreezing at −20 °C. Liq.N_2 freezing resulted in a chalky-white appearance in agreement with Farkas and Singh (1991), which was caused by the presence of tiny cavities that highly reflected or scattered light. The results indicated marked color changes (ΔE value) of freeze-dried soybean curd following Liq.N_2 freezing. The results suggested that modification of matrix structures, (i.e. the size of pore networks) effectively influenced the optical properties of freeze-dried matrices. Similarly, the a* and b*, which indicate redness and yellowness, increased as a result of freeze-drying; however, Liq.N_2 freezing caused diverse results with sharply decreased a* and b* values. Freezing at −90 °C caused an insignificant change in yellowness. Fig. 10 shows that the soybean curd systems could be grouped into three categories according to cluster analysis. Moreover, the rehydration could not recover the original color properties in the freeze-dried soybean curd prefrozen at −20 °C and −50 °C in agreement with Moreira et al. (2008). However, the rehydration of −90 °C and Liq.N_2 systems effectively recovered color and showed similar values to that of raw materials.

4. Conclusion

The cooling rates and freezing time effectively modified microstructural properties (the network integrity, pore size and wall thickness) of freeze-dried soybean curd. The microstructure

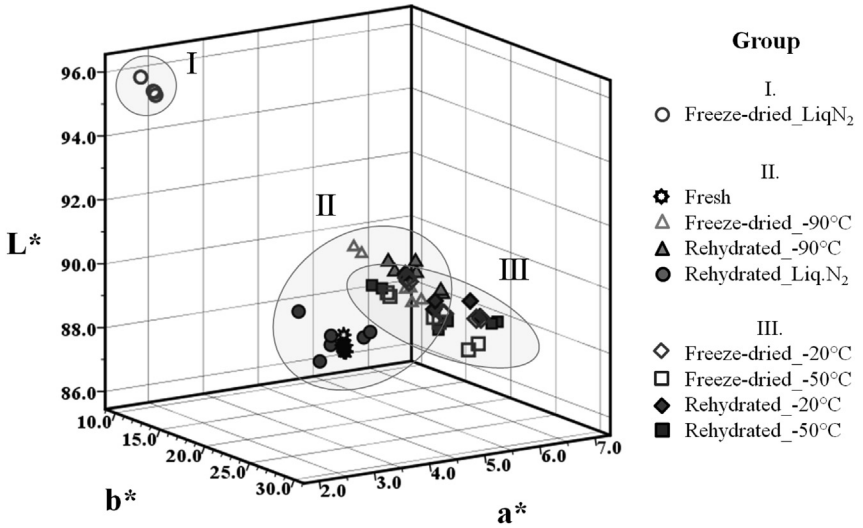

Fig. 10. Scatter plots for color properties (L*, a* and b*) of fresh, freeze-dried and rehydrated tofu prefrozen at −20 °C, −50 °C, −90 °C and in liq.N_2). Each system was determined for 6 measurements. Circles with different Roman numerals (I, II and III) distinguish groups resulting from multivariate statistical cluster analysis.

subsequently controlled the rehydration properties (the kinetics, solid loss and color of solids). Microstructural analysis (SEM and X-ray CT) clearly revealed that faster ice nucleation concurrent with a reduced freezing time limited ice growth and contributed to smaller pore sizes and lower wall thickness. Faster freezing and the resultant smaller pore size initially facilitated the rehydration rate. However, the rehydration subsequently decreased due to the high number of entrapped air bubbles. The large ice formation also disintegrated the protein networks and caused higher protein aggregation resulting in a thicker solid membrane. Water accessibility through solids was limited in the thicker networks because there was less water uptake at equilibrium under higher-temperature freezing conditions. Liq.N_2 freezing conditions effectively retained the microstructural properties and the original color could be recovered in the rehydrated soybean curd matrices. However, cracking was a severe problem as a result of very rapid freezing. The results indicated the relationship between the process-structure-rehydration properties in freeze-drying. The optimized freezing effectively improve water transport and the microstructural properties of freeze-dried food solids.

Acknowledgement

This work has been financial supported from Ministry of Education, Culture, Sports, Science and Technology (Japan) under “MEXT Revitalization Project for the creation of Fisheries Research and Education Center in Sanriku”. The authors are gratefully acknowledged Miss Yuri Kominami for the support on the SEM and fluorescence microscopic measurements.

References

Acevedo, N.C., Briones, V., Buera, P., Aguilera, J.M., 2008. Microstructure affects the rate of chemical, physical and color changes during storage of dried apple discs. J. Food Eng. 85 (2), 222–231.
Babić, J., Cantalejo, M.J., Arroqui, C., 2009. The effects of freeze-drying process parameters on *Broiler* chicken breast meat. LWT-Food Sci. Technol. 42 (8), 1325–1334.
Datta, A.K., 2007. Porous media approaches to studying simultaneous heat and mass transfer in food processes. I: problem formulations. J. Food Eng. 80 (1), 80–95.
Farkas, B.E., Singh, R.P., 1991. Physical properties of air-dried and freeze-dried chicken white meat. J. Food Sci. 56 (3), 611–615.
García-Pascual, P., Sanjuán, N., Melis, R., Mulet, A., 2006. *Morchella esculenta* (morel) rehydration process modelling. J. Food Eng. 72 (4), 346–353.
Harnkarnsujarit, N., Charoenrein, S., 2011. Influence of collapsed structure on stability of β-carotene in freeze-dried mangoes. Food Res. Int. 44 (10), 3188–3194.
Harnkarnsujarit, N., Charoenrein, S., Roos, Y.H., 2012. Microstructure formation of maltodextrin and sugar matrices in freeze-dried systems. Carbohydr. Polym. 88 (2), 734–742.
Hung, Y.C., 1997. Freeze-cracking. In: Erickson, M.C., Hung, Y.C. (Eds.), Quality in Frozen Food. Chapman & Hall, New York, USA.
Kang, H.W., Tabata, Y., Ikada, Y., 1999. Fabrication of porous gelatin scaffolds for tissue engineering. Biomaterials 20 (14), 1339–1344.
Keshun, L., 1997. Soybeans: Chemistry, Technology, and Utilization. Chapman & Hall.
Krokida, M.K., Marinos-Kouris, D., 2003. Rehydration kinetics of dehydrated products. J. Food Eng. 57 (1), 1–7.
Krokida, M.K., Philippopoulos, C., 2005. Rehydration of dehydrated foods. Dry. Technol. 23 (4), 799–830.
Kuprianoff, J., 1962. Some factors influencing the reversibility of freeze-drying of foodstuffs. Freeze-Drying Foods 16.
Lewicki, P.P., 1998. Effect of pre-drying treatment, drying and rehydration on plant tissue properties: a review. Int. J. Food Prop. 1 (1), 1–22.
Lin, T.M., Durance, T.D., Scaman, C.H., 1998. Characterization of vacuum microwave, air and freeze dried carrot slices. Food Res. Int. 31 (2), 111–117.
López-Leiva, M., Hallström, B., 2003. The original Plank equation and its use in the development of food freezing rate predictions. J. Food Eng. 58 (3), 267–275.
Ma, P.X., Zhang, R., 1999. Synthetic nano-scale fibrous extracellular matrix. J. Biomed. Mater. Res. 46, 60–72.
Marabi, A., Saguy, I.S., 2004. Effect of porosity on rehydration of dry food particulates. J. Sci. Food Agric. 84 (10), 1105–1110.
Marabi, A., Dilak, C., Shah, J., Saguy, I.S., 2004. Kinetics of solids leaching during rehydration of particulate dry vegetables. J. Food Sci. 69 (3), FEP91–FEP96.
Marques, L.G., Prado, M.M., Freire, J.T., 2009. Rehydration characteristics of freeze-dried tropical fruits. LWT-Food Sci. Technol. 42 (7), 1232–1237.
Meda, L., Ratti, C., 2005. Rehydration of freeze-dried strawberries at varying temperatures. J. Food Process Eng. 28 (3), 233–246.
Moreira, R., Chenlo, F., Chaguri, L., Fernandes, C., 2008. Water absorption, texture, and color kinetics of air-dried chestnuts during rehydration. J. Food Eng. 86 (4), 584–594.
O'Brien, F.J., Harley, B.A., Yannas, I.V., Gibson, L., 2004. Influence of freezing rate on pore structure in freeze-dried collagen-GAG scaffolds. Biomaterials 25 (6), 1077–1086.
Peighambardoust, S.H., Dadpour, M.R., Dokouhaki, M., 2010. Application of epi-fluorescence light microscopy (EFLM) to study the microstructure of wheat dough: a comparison with confocal scanning laser microscopy (CSLM) technique. J. Cereal Sci. 51 (1), 21–27.
Petzold, G., Aguilera, J.M., 2009. Ice morphology: fundamentals and technological applications in foods. Food Biophys. 4 (4), 378–396.
Rhim, J.W., Koh, S., Kim, J.M., 2011. Effect of freezing temperature on rehydration and water vapor adsorption characteristics of freeze-dried rice porridge. J. food Eng. 104 (4), 484–491.
Roos, Y., 1993. Melting and glass transitions of low molecular weight carbohydrates. Carbohydr. Res. 238, 39–48.
Roos, Y., Karel, M., 1991. Amorphous state and delayed ice formation in sucrose solutions. Int. J. Food Sci. Technol. 26, 553–566.
Saguy, I.S., Marabi, A., Wallach, R., 2005. New approach to model rehydration of dry food particulates utilizing principles of liquid transport in porous media. Trends Food Sci. Technol. 16 (11), 495–506.
Scherer, G.W., 1993. Freezing gels. J. Non-Cryst. Solids 155 (1), 1–25.
Voda, A., Homan, N., Witek, M., Duijster, A., van Dalen, G., van der Sman, R., Jaap Nijsse, J., van Vliet, L., Van As, H., van Duynhoven, J., 2012. The impact of freeze-drying on microstructure and rehydration properties of carrot. Food Res. Int. 49, 687–693.
Wallach, R., Troygot, O., Saguy, I.S., 2011. Modeling rehydration of porous food materials: II. The dual porosity approach. J. Food Eng. 105 (3), 416–421.
Wang, W., Nema, S., Teagarden, D., 2010. Protein aggregation—pathways and influencing factors. Int. J. Pharm. 390 (2), 89–99.
Witrowa-Rajchert, D., Lewicki, P.P., 2006. Rehydration properties of dried plant tissues. Int. J. Food Sci. Technol. 41 (9), 1040–1046.